


Diet-induced dyslipidemia induces metabolic and migratory adaptations in regulatory T cells

Jacob Amersfoort ^{1*}, Frank H. Schaftenaar ¹, Hidde Douna¹, Peter J. van Santbrink¹, Gijs H.M. van Puijvelde¹, Bram Slütter¹, Amanda C. Foks ¹, Amy Harms ², Estefania Moreno-Gordaliza ², Yanyan Wang³, Thomas Hankemeier², Ilze Bot ¹, Hongbo Chi³, and Johan Kuiper¹

¹Division of BioTherapeutics, LACDR, Leiden University, Einsteinweg 55, 2333 CC Leiden, The Netherlands; ²Division of Biomedicine and Systems Pharmacology, LACDR, Leiden University, Leiden, The Netherlands; and ³Department of Immunology, St. Jude Children's Research Hospital, Memphis, TN, USA

Received 14 February 2020; revised 18 May 2020; editorial decision 30 June 2020; accepted 6 July 2020; online publish-ahead-of-print 11 July 2020

Aims

A hallmark of advanced atherosclerosis is inadequate immunosuppression by regulatory T (Treg) cells inside atherosclerotic lesions. Dyslipidemia has been suggested to alter Treg cell migration by affecting the expression of specific membrane proteins, thereby decreasing Treg cell migration towards atherosclerotic lesions. Besides membrane proteins, cellular metabolism has been shown to be a crucial factor in Treg cell migration. We aimed to determine whether dyslipidemia contributes to altered migration of Treg cells, in part, by affecting cellular metabolism.

Methods and results

Dyslipidemia was induced by feeding *Ldlr*^{-/-} mice a western-type diet for 16–20 weeks and intrinsic changes in Treg cells affecting their migration and metabolism were examined. Dyslipidemia was associated with altered mTORC2 signalling in Treg cells, decreased expression of membrane proteins involved in migration, including CD62L, CCR7, and S1Pr1, and decreased Treg cell migration towards lymph nodes. Furthermore, we discovered that diet-induced dyslipidemia inhibited mTORC1 signalling, induced PPAR δ activation and increased fatty acid (FA) oxidation in Treg cells. Moreover, mass-spectrometry analysis of serum from *Ldlr*^{-/-} mice with normolipidemia or dyslipidemia showed increases in multiple PPAR δ ligands during dyslipidemia. Treatment with a synthetic PPAR δ agonist increased the migratory capacity of Treg cells *in vitro* and *in vivo* in an FA oxidation-dependent manner. Furthermore, diet-induced dyslipidemia actually enhanced Treg cell migration into the inflamed peritoneum and into atherosclerotic lesions *in vitro*.

Conclusion

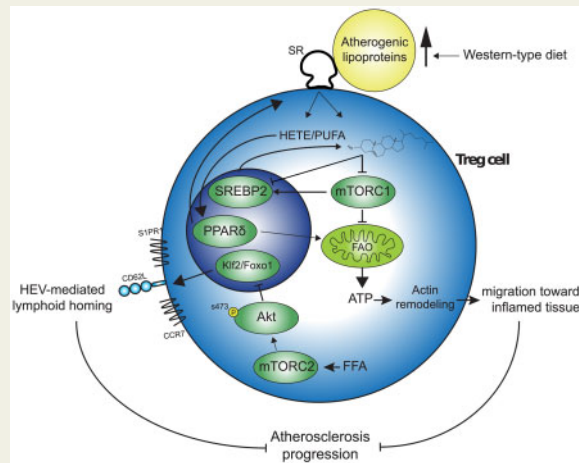
Altogether, our findings implicate that dyslipidemia does not contribute to atherosclerosis by impairing Treg cell migration as dyslipidemia associated with an effector-like migratory phenotype in Treg cells.

* Corresponding author. Tel: +31 71 5276213; E-mail: j.amersfoort@lacdr.leidenuniv.nl

© The Author(s) 2020. Published by Oxford University Press on behalf of the European Society of Cardiology.

This is an Open Access article distributed under the terms of the Creative Commons Attribution Non-Commercial License (<http://creativecommons.org/licenses/by-nc/4.0/>), which permits non-commercial re-use, distribution, and reproduction in any medium, provided the original work is properly cited. For commercial re-use, please contact journals.permissions@oup.com

Graphical Abstract



Keywords

Atherosclerosis • Dyslipidemia • Regulatory T cell • Metabolism • Migration

1. Introduction

Atherosclerosis is an autoimmune-like disease affecting the arterial wall in which (modified) lipoproteins, such as low-density lipoprotein (LDL) accumulate in the subendothelial space and elicit an adaptive immune response involving CD4⁺ T cells.¹ Dyslipidemia as exemplified by hypercholesterolemia and/or hypertriglyceridemia is a driving force for the development of atherosclerosis. A disease in which this is epitomized is familial hypercholesterolemia (FH), which is an inherited disease with a prevalence of 1 in 500 individuals worldwide^{2,3} and is characterized by dyslipidemia and premature cardiovascular disease (CVD). Given the autoimmune-like nature of atherosclerosis, immunomodulation has enormous potential as a therapy for CVD. Regulatory T (Treg) cells represent a subset of CD4⁺ T cells which maintains tolerance to self-antigens and regulates inflammation to dampen tissue damage.⁴ Treg cells are thus considered a promising therapeutic target to treat autoimmune-like disorders, including atherosclerosis.⁵ Accordingly, as Treg cell abundance is low in advanced atherosclerotic lesions in mice⁶ and humans,⁷⁻⁹ a local loss of tolerance to lipoproteins is speculated to be causal in atherosclerosis progression.

The capacity of Treg cells to bind to activated endothelium is inversely related to the degree of diet-induced dyslipidemia, presumably through decreased expression of ligands for P- and E-selectin on Treg cells.⁶ Thereby, fewer Treg cells which egress from secondary lymphoid organs (SLOs) can migrate towards atherosclerotic lesions, thereby contributing to a local loss of tolerance. Diet-induced dyslipidemia likely also affects Treg cell migration through a distinct mechanism. Specifically, obesity-induced lipid accumulation and metabolic stress primes CD4⁺ T cells to acquire an effector phenotype by altering mammalian target of rapamycin complex 2 (mTORC2) activity in the PI3K-p110δ-Akt kinase signalling pathway. This alteration lowers the expression of CD62L and C-C chemokine receptor type 7 (CCR7)¹⁰ which are involved in the

homing of T cells to lymph nodes (LNs) through high endothelial venules. Thus, dyslipidemia potentially modulates Treg cell migration by affecting the membrane expression of proteins required for their migration to sites of inflammation and LNs.

Recently, it was discovered that Treg cells also adapt their metabolism during inflammation and require glycolysis to generate sufficient ATP for their migration.¹¹

Dyslipidemia could affect Treg cell migration by affecting the cellular metabolism of Treg cells. Cholesterol accumulation in ATP-binding cassette G1 (ABCG1)-deficient Treg cells inhibits mTORC1.¹² mTORC1 can regulate cellular metabolism by promoting glycolysis in T cells through its downstream targets hypoxia inducible factor-1α (HIF1α) and Myc.^{13,14} Moreover, mTORC1 can inhibit fatty acid (FA) oxidation, by inhibiting the rate-limiting enzyme carnitine-palmitoyl transferase 1A (Cpt1a).^{15,16} Additionally, dyslipidemia can affect cellular metabolism in Treg cells through the lipid-induced activation of peroxisome proliferator activated receptors (PPARs), a class of lipid-activated transcription factors which can modulate cellular metabolism.¹⁷

Altogether, these reports indicate that key regulators of cellular metabolism and migration in Treg cells can be affected by perturbations in the levels of extra- and intracellular lipids.

In this article, we used *Ldlr*^{-/-} mice to investigate dyslipidemia-induced effects on the migratory phenotype and cellular metabolism of Treg cells residing in SLO. We discovered that dyslipidemia induced intrinsic changes in mTOR signalling and glycolysis, and increased PPARδ target gene expression and FA oxidation in splenic Treg cells. Dyslipidemia increased the capacity of Treg cells to migrate towards sites of inflammation and the PPARδ agonist GW501516 increased their migration in an FA oxidation-dependent manner. These results indicate that dyslipidemia can induce an effector-like migratory phenotype in Treg cells residing in specific SLOs, in part by skewing their metabolism, possibly leading to an increased potency to migrate towards sites of inflammation.

2. Methods

2.1 Mice

Diet-induced dyslipidemia and atherosclerosis were established by feeding *Ldlr*^{-/-} mice from 9 to 12 weeks of age a western-type diet (WTD) containing 0.25% cholesterol and 15% cocoa butter (Special Diet Services) for 16–20 weeks (unless stated otherwise). The animals were otherwise kept under standard laboratory conditions and were fed a normal chow diet (NCD) and water *ad libitum*. At sacrifice, the mice were anaesthetized by subcutaneous injections with ketamine (100 mg/mL), sedazine (25 mg/mL), and atropine (0.5 mg/mL). The mice were euthanized while sedated by disrupting their perfusion, as is described in the [Supplementary material online, Experimental Procedures](#). Alternatively, the mice were euthanized while sedated by cervical dislocation, depending on the organs which were harvested. All animal work was performed according to the guidelines of the European Parliament Directive 2010/63EU and the experimental work was approved by the animal ethics committee of Leiden University.

2.2 Flow cytometry

Spleens and lymph nodes were mashed through a 70 µm cell strainer after isolation. For the staining of surface markers, cells were stained at 4°C for 30 min in staining buffer [PBS with 2% (vol/vol) foetal bovine serum (FBS)] in which we diluted the antibodies. Intracellular transcription factors were stained for by following the FoxP3 staining protocol (eBioscience, Santa Clara, CA, US.). Filipin III (Cayman Chemicals, Ann Arbor, MI, USA) and BodipyTM (Thermo Fisher, Waltham, MA, USA) staining for cellular lipids (details in [Supplementary material online, Experimental Procedures](#)) was quantified in CD4⁺CD25⁺ Treg cells, of which ±95% expressed FoxP3 in SLOs (data not shown). For phosphorylated proteins, cells were fixed with BD PhosflowTM Lyse/Fix Buffer (BD Biosciences) and subsequently permeabilized with Phosflow Perm buffer III (BD Biosciences, Franklin Lakes, NJ, USA). Flow cytometric analysis was performed on a FACSCantoll (BD Biosciences) or a Cytoflex S (Beckman Coulter, Brea, CA, USA) and data were analysed using Flowjo software (TreeStar, Ashland, OR, USA).

2.3 Cell culture

Treg cells were stimulated using plate-coated anti-CD3e (5 µg/mL; eBioscience), anti-CD28 (0.5 µg/mL; eBioscience), and 200 U/mL recombinant mIL-2 (Peprotech) and cultured in RPMI-1640 supplemented with 2 mM L-glutamine, 100 U/mL pen/strep and 10% FBS (all from Lonza). *In vitro* lipid loading experiments were performed by supplementing culture medium with 10% mouse serum from *Ldlr*^{-/-} mice with normolipidemia or dyslipidemia. Alternatively, lipid loading was achieved by culturing Treg cells with β-very LDL particles. Etomoxir was used at 100 µM, which has no off-target effects on oxidative phosphorylation.¹⁸

2.4 RNA and immunoblot analysis

RNA isolation was performed using the guanidium isothiocyanate method after which cDNA was generated using RevertAid M-MuLV reverse transcriptase per manufacturer's instructions (Thermo Fisher). Quantitative gene expression analysis was performed using Power SYBR Green Master Mix on a 7500 Fast Real-Time PCR system (Applied Biosystems, Foster City, CA, USA). Gene expression was determined using the ddCt method. Immunoblot analysis was performed as described previously.¹⁹

2.5 FA oxidation assay

Freshly isolated or cultured Treg cells were incubated for 2 h (unless otherwise stated) at 37°C after which the supernatant was transferred to 20 mL scintillation vials which were sealed with a rubber stopper containing Whatman filtration paper pre-equilibrated in milliQ. After 48 h of incubation at 37°C, the Whatman filtration paper containing the metabolized ³H₂O was harvested. More details on this assay are provided in the supplements.

2.6 Metabolic flux assay

OCR and extracellular acidification rate (ECAR) were measured using an XF96e Extracellular Flux Analyzer (Seahorse Bioscience, North Billerica, MA, USA) per manufacturer's instructions.

2.7 Treg cell peritoneum migration

Treg cell peritoneum migration was based on Fu *et al.*²⁰ and performed as described previously.

2.8 Aorta influx

Aortic Treg cell influx was examined based on Li *et al.*²¹ and performed as described previously.

2.9 Transmigration assay

Treg cells were applied to transwell tissue culture well inserts (5 µm pore-size) and left to migrate towards 250 ng/mL CCL21 (Peprotech, London, UK) for 6–8 h. The number of migrated cells was determined manually using a haemocytometer.

2.10 Serum analysis

Concentrations of total cholesterol and triglycerides in the serum were determined using a colorimetric assay. Concentrations of free FAs in the serum were quantified using the Free Fatty Acid Quantification Kit (Sigma) as per manufacturer's instructions. Mice were fasted for 4 h prior to blood collection for measurement of blood glucose levels. Blood samples were taken from the tail vein and directly applied to an Accu-Check glucometer (Roche Diagnostics, Mannheim, Germany).

2.11 Serum lipidomics

Ldlr^{-/-} mice were fed a WTD or maintained on an NCD for 8 weeks and upon sacrifice, serum samples were collected and frozen at -80°C until use. The operating procedures of the targeted lipidomics platform are optimized from the previously published method.²² The leukotrienes, hydroxyl-FAs, epoxy-FAs, and lipoxins were analysed using a fully targeted method as previously described.²³

2.12 Suppression assay

Treg cells were isolated and co-cultured in complete RPMI with splenocytes labelled with 5 µM CellTrace Violet. The cells were stimulated with anti-CD3e (1 µg/mL; eBioscience), anti-CD28 (0.5 µg/mL; eBioscience), and 100 U/mL recombinant mIL-2 (Peprotech). The suppressive capacity of Treg cells was determined by flow cytometry by measuring the proliferation of CellTrace Violet labelled CD4⁺ T effector cells after 72 h in different Treg: splenocyte ratios in which the amount of splenocytes per well were set at 50 000 cells.

2.13 Statistical analysis

A two-tailed Student's *t*-test was used to compare individual groups with Gaussian distributed data. Correction for multiple comparisons was

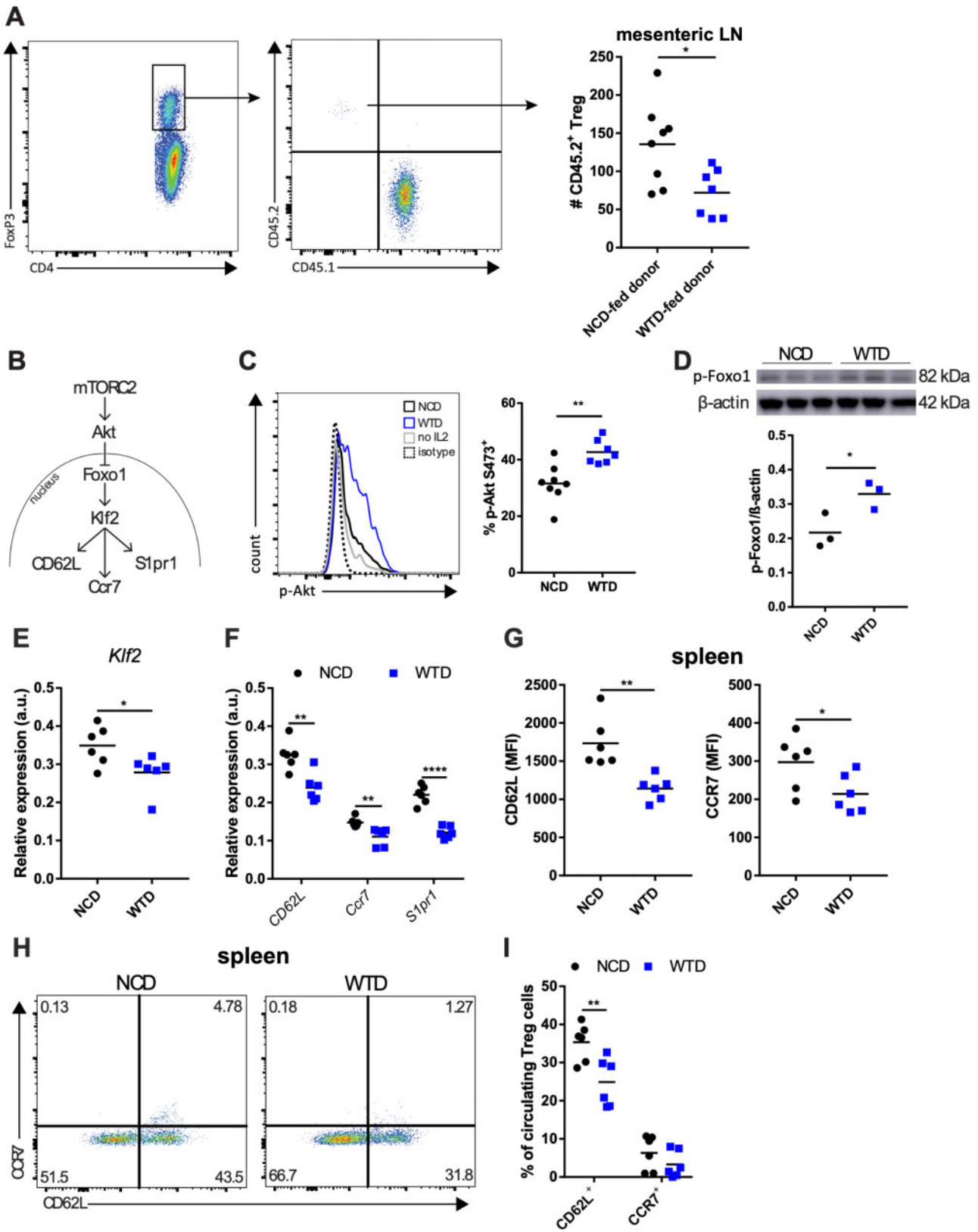


Figure 1 Diet-induced dyslipidemia in *Ldlr*^{-/-} mice increases mTORC2 activity and decreases lymph node homing of splenic Treg cells. (A) Quantification of adoptively transferred Treg cells in mesenteric LN in a peritoneal homing experiment. CD4⁺ donor T cells were adoptively transferred and the presented Treg cell number is normalized for the number of Treg cells which was present in each CD4⁺ donor cell fraction. *n* = 7–8 mice/group. (B) mTORC2-Akt-Foxo1-Klf2 axis. (C) Representative plot of p-Akt detection by flow cytometry (left panel) and percentage of p-Akt⁺ cells in splenic Treg cells from NCD-fed (NCD-Treg cells) or WTD-fed mice (WTD-Treg cells). *n* = 7–8 mice/group. (D) Representative immunoblot and quantification of p-Foxo1 levels in

performed using Bonferroni correction. Non-parametric data were analysed using a Mann–Whitney *U*-test. Data from three groups were analysed using a one-way analysis of variance (ANOVA) with a subsequent Tukey's multiple comparison test. A *P*-value below 0.05 was considered significant. In the figures * indicates *P* < 0.05, ** indicates *P* < 0.01, *** indicates *P* < 0.001, and **** indicates *P* < 0.0001.

3. Results

3.1 Diet-induced dyslipidemia alters mTORC2 signalling and decreases Treg cell LN homing

To study alterations in Treg cell metabolism and migration in the context of dyslipidemia and atherosclerosis, NCD fed *Ldlr*^{-/-} mice were compared to *Ldlr*^{-/-} mice which were fed a WTD for 16–20 weeks. WTD-fed mice develop advanced atherosclerotic lesions with a low abundance of Treg cells⁶ and metabolic dysregulation in the form of hypercholesterolemia (Supplementary material online, Figure S1A) and hypertriglyceridemia (Supplementary material online, Figure S1B) but not hyperglycemia (Supplementary material online, Figure S1C).

We first examined whether WTD-induced dyslipidemia changes LN migration of splenic Treg cells as dyslipidemia affects CD62L expression in this Treg cell compartment.⁶

A peritoneal homing experiment²⁰ was performed using isolated splenic CD4⁺ T cells from NCD- or WTD-fed donor *Ldlr*^{-/-} mice which were injected i.v. into CD45.1 acceptor mice and the number of donor Treg cells (normalized for the number of injected Treg cells) in mesenteric LNs were quantified. We observed that fewer Treg cells from WTD-fed mice (WTD-Treg cells) had migrated towards mesenteric LNs compared with Treg cells from NCD-fed mice (NCD-Treg cells) (Figure 1A). Interestingly, the number of donor conventional T (Tconv) cells which had migrated into the mesenteric LNs was equal in both diet-groups (Supplementary material online, Figure S1D). We postulated that, similar to CD4⁺ effector T cells in obesity, the observed decrease in LN homing was caused by metabolic stress in Treg cells which increased mTORC2 activity. Through phosphorylation of Akt kinase at the serine 473 residue²⁴ and subsequent phosphorylation of forkhead Box O1 (Foxo1), increased mTORC2 activity decreases the expression of *Klf2*, *CD62L*, *CCR7*, and *S1pr1*, as suggested in Figure 1B. *Klf2* encodes Krüppel-like factor 2 which, like Foxo1, is a transcription factor whose target genes include *CD62L*, *CCR7*, and sphingosine-1-phosphate receptor 1 (*S1Pr1*).²⁴ The percentage p-Akt S473 expressing Treg cells was elevated in WTD-Treg cells as compared to NCD-Treg cells (Figure 1C). The percentage of p-Akt S473 expressing splenic Tconv cells was also increased in WTD-fed mice (Supplementary material online, Figure S1E), though this effect was ~30-fold smaller than in Treg cells.

In WTD-Treg cells, levels of p-Foxo1, reflecting Foxo1 excluded from the nucleus,²⁴ were elevated (Figure 1D). The decreased *Klf2* expression (Figure 1E) could, together with less nuclear Foxo1, explain the

decreased expression of *CD62L*, *Ccr7*, and *S1pr1* observed in WTD-Treg cells (Figure 1F). We observed, using flow cytometry, decreased protein expression of *CD62L* and *CCR7* (Figure 1G) and a decreased percentage of Treg cells expressing *CD62L* and/or *CCR7* (Figure 1H) in splenic WTD-Treg cells. Interestingly, the percentage of CD44⁺ (Supplementary material online, Figure S1F) or CD69⁺ Treg cells (Supplementary material online, Figure S1G) and *Ccr2* and *Ccr5* expression in Treg cells (Supplementary material online, Figure S1H) were unaffected by diet-induced dyslipidemia, suggesting that mostly the LN homing genes were affected. Lastly, the percentage of circulating CD62L⁺ Treg cells was ~10% lower in WTD-mice as compared to NCD-mice (Figure 1I).

Overall, these data indicate that, similar to diet-induced obesity, WTD-induced dyslipidemia caused intrinsic changes in mTORC2 activity in Treg cells and decreased the capacity of Treg cells to migrate towards LNs.

3.2 Diet-induced dyslipidemia increases lipids and inhibits mTORC1 activity in WTD-Treg cells

Next, we characterized lipid accumulation of Treg cells in various SLOs and the circulation.

First, we examined the cholesterol levels in Treg cells in the blood, spleen, draining LN (mediastinal, medLN), and non-draining LN (inguinal, iLN) in NCD- and WTD-fed *Ldlr*^{-/-} mice using filipin staining. WTD-Treg cells in spleen and medLN showed cholesterol accumulation whereas Treg cells in the blood and iLN were unaffected (Figure 2A). Cholesterol accumulation after 4 weeks of WTD (where the inflammatory response is not at its peak in *Ldlr*^{-/-} mice) was observed specifically in Helios⁺ Treg cells (Supplementary material online, Figure S2A), suggesting that lipid accumulation may be subset specific.²⁵

The percentages of Treg cells in spleen and medLN were increased after 16–20 weeks of WTD (Figure 2B), which might be caused by proliferation in an earlier stage of atherosclerosis. In the spleen, this increase in the percentage of Treg cells resulted in a strongly expanded splenic Treg cell population (Figure 2C). Furthermore, dyslipidemia associated with lipid droplet accumulation in Treg cells in the spleen and medLN (Figure 2D). Given the extent of lipid accumulation and the size and relevance of this population, we specifically used splenic Treg cells for more extensive molecular, metabolic and functional characterization. Hence, when comparing NCD- and WTD-Treg cells we refer to Treg cells isolated from spleens of *Ldlr*^{-/-} mice fed an NCD or WTD, respectively, unless explicitly stated otherwise.

In line with cholesterol accumulation, mTORC1 activity, reflected by phosphorylated (p)-S6 levels, was lower in WTD-Treg cells than in NCD-Treg cells as measured by flow cytometry (Figure 2E) and immunoblot (Figure 2F). In addition, mRNA expression of *Srebp1* and *Srebp2*, which is decreased by inhibition of mTORC1^{26,27} and whose activity is decreased in conjunction with mTORC1 upon increased lysosomal- and endoplasmic reticulum-cholesterol levels,²⁸ was diminished in WTD-

Figure 1 Continued

NCD- and WTD-Treg cells. *n* = 3 mice/group. (E) *Klf2* mRNA expression and (F) mRNA expression of *CD62L*, *Ccr7* and *S1pr1* in NCD- and WTD-Treg cells. *n* = 6 mice/group. (G) MFI for *CD62L* and *CCR7* on NCD- and WTD-Treg cells. *n* = 6 mice/group. (H) Representative plots of percentages of *CD62L*⁺ and *CCR7*⁺ from the experiment in G. (I) *CD62L* and *CCR7* expression in Treg cells in the blood of NCD- and WTD-fed mice. *n* = 6 mice/group. A two-tailed Student's *t*-test was used. **P* < 0.05, ***P* < 0.01, ****P* < 0.001, and *****P* < 0.0001. A represents one experiment. C–H are representative data for two independent experiments. MFI, median fluorescence intensity.

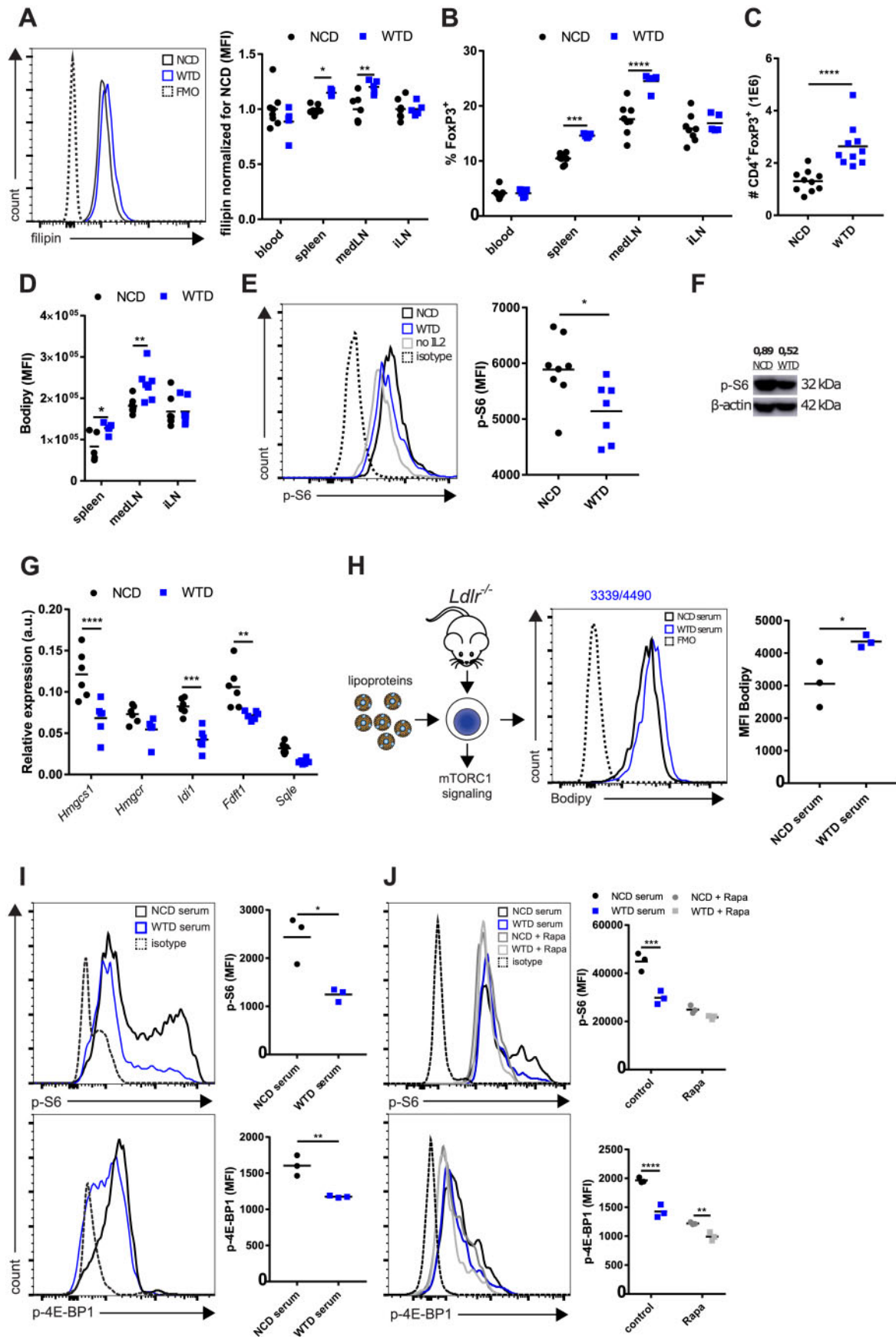


Figure 2 mTORC1 activity is diminished in Treg cells from WTD-fed *Ldlr*^{-/-} mice. (A) Filipin staining for cholesterol in CD4⁺CD25⁺ Treg cells from blood, spleen, mediastinal lymph node (medLN), and inguinal lymph node (iLN) of NCD- and WTD-fed *Ldlr*^{-/-} mice. Normalized per tissue for the NCD

Treg cells (Supplementary material online, Figure S2B). The expression of enzymes which are crucially involved in cholesterol synthesis through the mevalonate pathway was decreased at an mRNA level (Figure 2G). In particular, *Hmgcs1*, *Idi1*, and *Fdft1* mRNA expression was decreased by ~50% (Figure 2G). Next, we measured suppressive capacity of NCD- and WTD-Treg cells as Treg cells lacking Raptor, an essential protein in mTORC1, lose their suppressive capacity due to reduced activity of the mevalonate pathway.¹⁹ NCD-Treg cells and WTD-Treg cells had similar capacity to suppress proliferation of CD4⁺ T effector cells (Supplementary material online, Figure S2C). In line, no differences were observed in the percentage of ICOS⁺ Treg cells (Supplementary material online, Figure S2D) and *Il10* and *Tgfb* mRNA expression (Supplementary material online, Figure S2E), though there was a slight increase in CTLA-4⁺ (Supplementary material online, Figure S2F) cells in WTD-Treg cells as compared to NCD-Treg cells. mTORC1 activity as measured by p-S6 levels was also decreased in Tconv cells from WTD-fed mice (Supplementary material online, Figure S2G) indicating that mTORC1 signalling in non-Treg cells can also be affected by dyslipidemia.

Subsequently, we aimed to mimic dyslipidemia *in vitro* by culturing Treg cells in medium supplemented with serum from NCD or WTD-fed mice, or with isolated β -very low-density lipoprotein (β -VLDL) (Figure 2H), thereby increasing cholesterol load without lipotoxicity-induced apoptosis as can occur with oxidized LDL (oxLDL).²⁹ Lipid loading *in vitro* through serum supplementation mimicked the effects of hypercholesterolemia on mTORC1 activity as measured by levels of p-S6 and p-4E-BP1 (an additional mTORC1 target) levels in Treg cells (Figure 2I). Importantly, this effect of serum supplementation also occurred in Treg cells isolated from C57/BL6 mice and was mTOR-dependent, as preincubation with rapamycin (an mTOR inhibitor) severely diminished the WTD-serum induced inhibition of mTORC1 activity (Figure 2J). Additionally, p-S6 was reduced by ~50% when incubating Treg cells with isolated β -VLDL (Supplementary material online, Figure S2H).

Altogether, these results showed that dyslipidemia induced lipid accumulation in Treg cells and reduced mTORC1 activity and the expression of genes crucially involved in the mevalonate pathway, without altering their suppressive capacity.

3.3 WTD-Treg cells have impaired glycolysis but increased FA oxidation

Next, we reasoned that dyslipidemia-induced mTORC1 inhibition would change the bioenergetic metabolism in WTD-Treg cells and measured glycolysis in NCD- and WTD-Treg cells using an XF analyzer. We observed a decrease in the basal ECAR in WTD-Treg cells (Figure 3A),

reflecting decreased lactate producing glycolysis. Furthermore, WTD-Treg cells had decreased glycolytic reserve and glycolytic capacity upon exposure to the complex I inhibitor oligomycin (Figure 3B). We observed a decrease in mRNA expression of the target genes of HIF1 α and Myc (*Glut1*, *Pgk1*, *LDHa*, *Pkm2*) when culturing Treg cells with WTD serum *in vitro* (Supplementary material online, Figure S3A). However, immunoblot analysis revealed that HIF1 α levels were unchanged (Supplementary material online, Figure S3B) as were the mRNA expression levels of *Glut1*, *Pgk1*, *LDHa*, *Pkm2* (Supplementary material online, Figure S3C) in freshly isolated WTD-Treg cells as compared to NCD-Treg cells. Similar to HIF1 α , Myc can transcriptionally regulate the expression of glycolytic genes¹⁴; however, Myc protein levels were equal between NCD- and WTD-Treg cells (Supplementary material online, Figure S3D). We speculate that, as the Treg cells, we used were preactivated, mTORC1 inhibition affected glycolysis only upon activation as mTORC1 activity is strongly increased upon activation.¹⁹

mTORC1 can also promote mitochondrial biogenesis,³⁰ but the mitochondrial mass in Treg cells was equal in both groups (Figure 3C). In line, the OCR, a measure for oxidative phosphorylation, showed no differences between NCD-Treg cells and WTD-Treg cells (Figure 3D), implicating diet-induced dyslipidemia did not affect mitochondrial function.

As mTORC1 can modulate FA oxidation through *Cpt1*, we next studied FA oxidation in Treg cells by measuring the detritiation of ³H-palmitic acid. Rapamycin increased mitochondrial FA oxidation in Treg cells as compared to the control (Supplementary material online, Figure S3E). In line with dyslipidemia-induced mTORC1 inhibition, isolated WTD-Treg cells displayed twice the level of mitochondrial FA oxidation (Figure 3E) and a comparable increase in *Cpt1a* expression (Figure 3F). Importantly, FA oxidation in Tconv cells was unaffected (Supplementary material online, Figure S3F). Although CPT1 deficient Treg cells proliferate normally,¹⁸ mitochondrial FA oxidation has also been shown to regulate Treg cell proliferation.³¹ Importantly, WTD-Treg cells were not more proliferative than NCD-Treg cells at this advanced timepoint of feeding mice a WTD (Supplementary material online, Figure S3G). To examine whether the metabolic adaptations in WTD-Treg cells were specifically linked to diet-induced dyslipidemia and not the chronic systemic low-grade inflammation which is associated with atherosclerosis,³² we performed a diet-switch experiment in which we reverted WTD-fed mice to an NCD. At 18 days after reverting the mice to an NCD, total cholesterol levels in the serum were normalized in the diet-switch group (Figure 3G). Accordingly, cholesterol levels were normalized in Treg cells from diet-switch mice (hereafter referred to as DS-Treg cells) (Figure 3H). In line, gene expression of liver-X-receptor (which is activated by cholesterol-derivatives) target genes *Abca1* and *Abcg1* was increased in WTD-Treg cells but not in DS-Treg cells (Figure 3I). We next

Figure 2 Continued

group. *n* = 5–8 mice/group. (B) Percentage of Treg cells in same tissues and groups as in (A). (C) Absolute number of Treg cells in spleen of NCD- or WTD-fed mice. *n* = 10 mice/group. (D) Bodipy staining for lipid droplets in CD4⁺CD25⁺ Treg cells. (E) p-S6 levels in splenic Treg cells from NCD-fed (NCD-Treg cells) or WTD-fed mice (WTD-Treg cells) as measured by flow cytometry. *n* = 7–8 mice/group. (F) p-S6 immunoblot of flow-sorted NCD- and WTD-Treg cells. p-S6 levels were normalized for β -actin levels as shown above the lanes. *n* = 1 mouse/group. (G) mRNA expression of genes from mevalonate pathway in NCD- and WTD-Treg cells. *n* = 6 mice/group. (H) *In vitro* lipid loading of Treg cells to study mTORC1 signalling. *n* = 3 mice/group. (I) p-S6 and p-4E-BP1 levels in isolated splenic *Ldlr*^{-/-} Treg cells after 48 h *in vitro* lipid loading with serum. *n* = 3 per group. Cells from three donor mice were used. (J) p-S6 and p-4E-BP1 levels after 48 h *in vitro* lipid loading of isolated wildtype splenic Treg cells with rapamycin and/or serum. *n* = 3 mice/group. Cells from three donor mice were used. A two-tailed Student's *t*-test was used. Non-parametric data were analysed using a Mann–Whitney *U*-test. **P* < 0.05, ***P* < 0.01, ****P* < 0.001, and *****P* < 0.0001. A–E and G–I are representative data for three individual experiments. J represents one experiment. K is representative for two individual experiments. FMO, fluorescence minus one control.

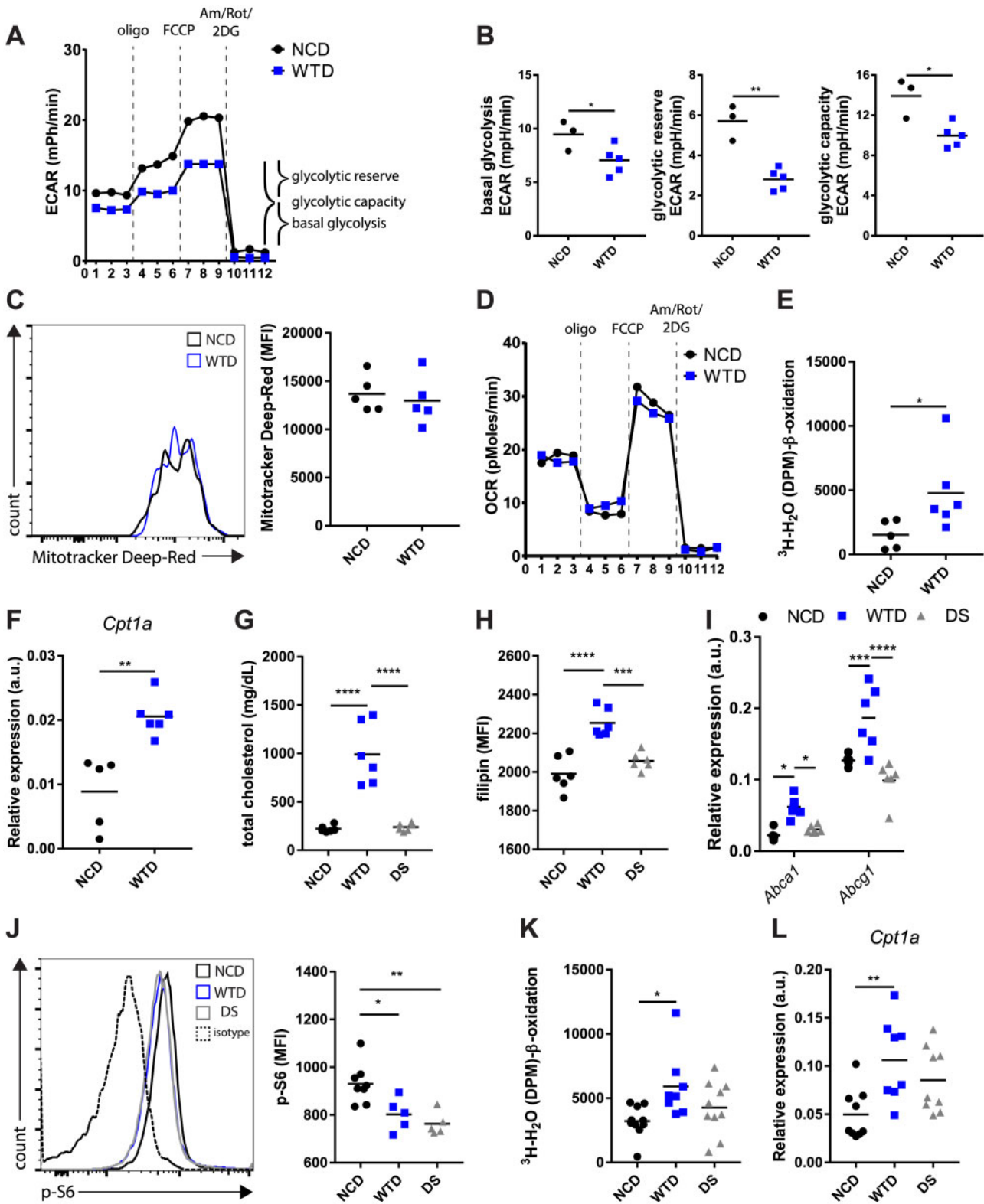


Figure 3 Diet-induced dyslipidemia in *Ldlr*^{-/-} mice impaired glycolytic metabolism but enhanced mitochondrial FA oxidation in WTD-Treg cells. (A) ECAR in NCD- and WTD-Treg cells in response to indicated compounds. *n* = 3–5 mice/group. (B) Basal glycolysis, glycolytic reserve, and glycolytic capacity quantified from (A). (C) Mitochondrial mass in isolated NCD- and WTD-Treg cells. *n* = 5 mice/group. (D) OCR in same assay as in (A). (E) ^3H -palmitic acid detritiation in isolated NCD- and WTD-Treg cells. *n* = 5–6 mice/group. (F) *Cpt1a* expression in isolated NCD- and WTD-Treg cells. *n* = 5–6 mice/group. (G) Total serum cholesterol levels in diet-switch experiment, examining NCD- and WTD-fed *Ldlr*^{-/-} mice as well as mice switched from a WTD to an NCD. *n* = 6 mice/group. (H) Filipin staining in NCD-, WTD-, and diet-switch (DS)-Treg cells. *n* = 6 mice/group. (I) mRNA expression of *Abca1* and *Abcg1* in NCD-, WTD-, and DS-Treg cells. *n* = 6 mice/group. (J) p-S6 levels as measured by flow cytometry in NCD-, WTD-, and DS-Treg cells. *n* = 5–8 mice/group. (K)

measured mTORC1 activity and FA oxidation to assess whether these were also normalized in Treg cells when WTD-fed mice are switched to an NCD. Strikingly, flow cytometric analysis revealed that mTORC1 activity in DS-Treg cells was diminished as compared to NCD-Treg cells (Figure 3J). This suggests that normalization of mTORC1 activity may occur gradually after normalization of cellular cholesterol levels. Remarkably, however, despite mTORC1 activity being attenuated, mitochondrial FA oxidation (Figure 3K) and *Cpt1a* expression in DS-Treg cells were equal to NCD-Treg cells (Figure 3L).

Collectively, these data indicate that glycolysis and FA oxidation are modulated in WTD-Treg cells but that the latter effect of dyslipidemia might not be exclusively mediated by mTORC1.

3.4 WTD increases PPAR δ ligands in serum and the expression of PPAR δ target genes in Treg cells

We sought to determine which additional mechanism(s) could contribute to increased *Cpt1a* expression and FA oxidation in WTD-Treg cells and reasoned that PPARs might be involved as these are activated by dietary lipids and can modulate glycolysis and FA metabolism.³³

We were unable to detect PPAR α expression in NCD- or WTD-Treg cells (Supplementary material online, Figure S4A). PPAR δ and PPAR γ share some of their target genes, but the mRNA expression of PPAR γ target genes *Scd1* and *Dgat* did not differ between NCD- and WTD-Treg cells (Supplementary material online, Figure S4B). Since PPAR γ target genes are involved in the uptake and biosynthesis of lipids and PPAR δ expression was about 10-fold higher compared to PPAR γ expression in Treg cells (Supplementary material online, Figure S4A), we focused on the role of PPAR δ .

We first examined PPAR δ activation in Treg cells and treated isolated Treg cells with GW501516, a PPAR δ agonist, *in vitro*. GW501516 treatment increased the expression of *Cpt1a*, *Slc25a20*, and *Plin2* while decreasing *Lipe* expression (Figure 4A). *Slc25a20* and *Plin2* expression were increased and *Lipe* expression was decreased in WTD-Treg cells as compared to NCD-Treg cells (Figure 4B), indicating that specific target genes of PPAR δ which are involved in FA catabolism (*Slc25a20*, *Lipe*) and lipid droplet formation (*Plin2*) were indeed modulated in WTD-Treg cells.

Long-chain FAs which are taken up via CD36, a scavenger receptor and transcriptional target of PPAR γ ,³⁴ modulate the activity of PPAR δ and expression of genes involved in FA- and glucose metabolism.³⁵ Compared to NCD-Treg cells, CD36 levels were increased on WTD-Treg cells but not DS-Treg cells (Supplementary material online, Figure S4C), suggesting that elevated CD36 expression might contribute to increased FA oxidation in WTD-Treg cells. CD36 expression in Tconv cells from WTD-fed mice was also increased but remained far lower as compared to Treg cells (Supplementary material online, Figure S4D). We performed metabolomics profiling by high-performance liquid chromatography and mass spectrometry of the free and total oxidized lipids in sera of NCD- and WTD-fed mice to quantify changes in PPAR δ ligand abundance. We selected previously described PPAR δ ligands^{36–38} in our lipidomics platform and examined relative changes in the serum of *Ldlr*^{-/-}

mice fed a WTD for 8 weeks. In general, PPAR δ ligands were increased in the dyslipidemia serum of WTD-fed *Ldlr*^{-/-} mice as compared to NCD control serum (Figure 4C). Especially saturated- and monounsaturated FAs (Figure 4D), hydroxyeicosatetraenoic acid (HETE) (Figure 4E), and lysophosphatidylcholine (Figure 4F) were increased in WTD serum. There were no changes in the abundance of serum prostaglandins (Figure 4G). HETEs can be synthesized from various polyunsaturated FAs, including arachidonic acid (AA), dihomo- γ -linolenic acid (DGLA), or eicosapentaenoic acid (EPA) through similar pathways. AA (20:4 ω -6) showed a 20% decrease in WTD serum as compared to NCD serum (Supplementary material online, Figure S4E). EPA was nearly undetected in WTD serum (Supplementary material online, Figure S4F) but DGLA was actually increased (Supplementary material online, Figure S4G), suggesting that increases in DGLA could have contributed to increased HETEs in WTD serum. Specific triglyceride-derived FAs, which were identified as potent natural ligands for PPAR δ but not for PPAR γ in macrophages,³⁶ were increased in WTD-serum, including palmitoleic, elaidic, eicosenoic, and erucic acid (Figure 4D). To observe whether free fatty acids (FFAs) and triglycerides indeed changed upon a DS (possibly explaining changes in *Cpt1a* expression) we measured their serum levels. Reverting WTD-fed mice to an NCD normalized the FFA levels in the serum (Supplementary material online, Figure S4H) as well as serum triglycerides (Supplementary material online, Figure S4I). Next, we tested whether PPAR δ activation could indeed explain increased gene expression of *Cpt1a*, *Plin2* and *Slc25a20* in WTD-Treg cells. We treated isolated NCD- and WTD-Treg cells *in vitro* with the PPAR δ antagonist/inverse agonist GSK0660 and observed that the increased mRNA expression of *Cpt1a* and *Plin2*, but not of *Slc25a20*, in WTD-Treg cells was sensitive to GSK0660 (Figure 4H). After 4 weeks of WTD, the expression of the PPAR δ target gene *Plin2* was elevated in WTD-Treg cells and the PPAR γ -antagonist T0070907 had no effect on its expression (Supplementary material online, Figure S4J), suggesting that the effects of prolonged dyslipidemia on lipid metabolism-associated genes might indeed be PPAR δ -mediated.

The presented data show that dyslipidemia increased the abundance of PPAR δ ligands in the circulation, thereby possibly increasing PPAR δ activity in Treg cells and contributing to increased FA oxidation.

3.5 Treg cells with high level of FA oxidation migrate more efficiently towards sites of inflammation

We explored whether changes in glycolytic- and FA metabolism affected WTD-Treg cell migration. We mimicked PPAR δ activation by dyslipidemia in primary Treg cells *in vitro* using the PPAR δ agonist GW501516 and assessed their migration in a peritoneal homing assay. Similar to WTD-Treg cells, mitochondrial FA oxidation was increased in GW501516-treated Treg cells compared with the control condition (Figure 5A). Additionally, GW501516 treatment decreased *Glut1* expression on Treg cells on an mRNA (Figure 5B) and protein level (Figure 5C). Importantly, the expression of membrane proteins involved in migration, including CCR5, CCR7 (the receptor for CCL21), CXCR3, CD62L, and

Figure 3 Continued

³H-palmitic acid detritiation after 4 h incubation with ³H-palmitic acid in NCD-, WTD-, and DS-Treg cells. *n* = 8–10 mice/group. (L) *Cpt1a* mRNA expression in NCD-, WTD-, and DS-Treg cells. *n* = 8–10 mice/group. Data were analysed using a two-tailed Student's *t*-test and a one-way ANOVA with a subsequent Tukey's multiple comparison test. **P* < 0.05, ***P* < 0.01, ****P* < 0.001, and *****P* < 0.0001. A–J represents data from two independent experiments. Data in K and L are pooled from two independent experiments showing similar effects. DS, diet switch group.

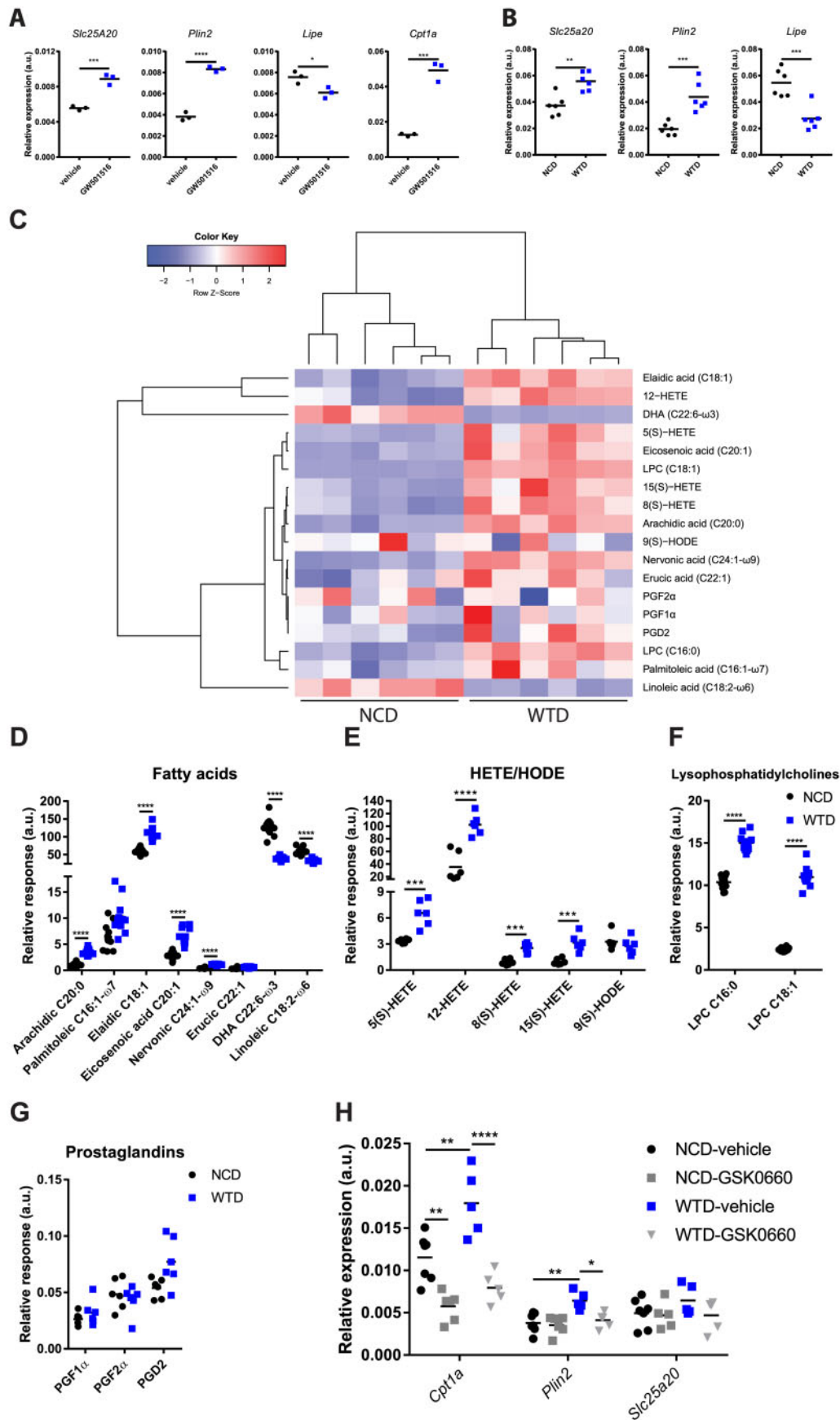


Figure 4 Diet-induced dyslipidemia in *Ldlr*^{-/-} mice increases circulating PPAR δ ligands and PPAR δ target gene expression in WTD-Treg cells. (A) mRNA expression of *Slc25a20*, *Plin2*, *Lipe*, and *Cpt1a* in flow-sorted Treg cells treated with GW501516 or vehicle *in vitro*. $n = 3$ mice/group. (B) mRNA expression of

LFA-1 were unaffected by GW501516-induced PPAR δ activation (Supplementary material online, Figure S5A). GW501516-treated Treg cells migrated more efficiently towards the inflamed peritoneum as compared to vehicle control (Figure 5D). Moreover, this effect was FA oxidation-dependent as preincubating GW501516-treated Treg cells with etomoxir (an irreversible CPT1 inhibitor) abolished it. Importantly, etomoxir did not affect Treg cell viability (Figure 5E). A transwell migration assay with CCL21 (the ligand for CCR7, whose expression was not affected by GW501516 thus allowing us to assess its metabolic effects) confirmed that GW501516-treated Treg cells displayed more potent migration, again in an FA oxidation-dependent fashion (Figure 5F). Next, as we unravelled a metabolic phenotype in WTD-Treg cells that might actually promote their migratory capacity, we assessed this in a peritoneal homing assay. Although the absolute number of migrated WTD-Treg cells was equal to NCD-fed donor derived Treg cell migration (Figure 5G), the percentage of WTD-Treg cells in the peritoneal Treg cell population was higher than NCD-Treg cells (Figure 5H). Supposedly, this was because the total number of Treg cells, which were recruited towards the inflamed peritoneum in the WTD-Treg cell-injected mice, was lower but the migratory capacity of WTD-Treg cells was higher than NCD-Treg cells. To study WTD-Treg cell migration in an atherosclerosis-specific context, we performed an *in vitro* aorta homing experiment using NCD- and WTD-Treg cells with or without preincubation with etomoxir. Indeed, WTD-Treg cells migrated more efficiently into atherosclerotic lesions as compared to NCD-Treg cells (Figure 5I). Here, as opposed to GW501516-treated Treg cells, the increased migratory capacity of WTD-Treg cells was only mildly affected by pretreatment with etomoxir.

In conclusion, these results indicate that PPAR δ -induced increases in FA oxidation potentiate Treg cell migration and that WTD-Treg cells might actually migrate more efficiently towards sites of inflammation.

3.6 Diet-induced dyslipidemia increases lipids in T cells from atherosclerotic lesions of *Ldlr*^{-/-} mice

Finally, we examined lipid-associated changes in Treg cells in atherosclerotic lesions. We assessed the amount of cholesterol and lipid droplets in CD4⁺CD25^{hi} T cells from atherosclerotic lesions of the aortic arches of NCD- and WTD-fed *Ldlr*^{-/-} mice (Figure 6A). In atherosclerotic lesions from aortic arches the amount of cholesterol (Figure 6B) and lipid droplets (Figure 6C) was, similar to the spleen and medLN, higher in CD4⁺CD25^{hi} T cells from WTD-fed mice as compared to NCD-fed mice. Again, similar to WTD-Treg cells, CD4⁺CD25^{hi} T cells from the atherosclerotic lesions of WTD-fed mice had increased expression of CD36 as compared to NCD controls (Figure 6D). Finally, we measured apoptosis of WTD-Treg cells as Treg cells inside atherosclerotic lesions are particularly apoptotic as atherosclerosis progresses, which is linked

to dyslipidemia.⁶ Indeed, Treg cells were more sensitive to rotenone-induced apoptosis than Tconv cells (Supplementary material online, Figure S6).

4. Discussion

A decrease in Treg cells in atherosclerotic lesions is associated with the degree of dyslipidemia. We showed that Treg cells accumulate cholesterol and other neutral lipids during dyslipidemia which, through intrinsic changes in mTORC1/mTORC2 signalling and PPAR δ activity, skewed their migration towards sites of inflammation instead of LNs. Pharmacological activation of PPAR δ with GW501516 mimicked the effects of dyslipidemia on FA oxidation in Treg cells and increased their migration towards sites of inflammation. These findings suggest that the decrease in Treg cell immunosuppression in advanced atherosclerosis is not due to dyslipidemia-induced impairments in migratory capacity as dyslipidemia actually induced an effector-like migratory phenotype in Treg cells, by biasing migration towards sites of inflammation.

An important point to address is how Treg cell-mediated immunosuppression is decreased in atherosclerotic lesions while diet-induced dyslipidemia induces intrinsic (metabolic) changes which skews their migratory phenotype, presumably in a beneficial manner. We propose that diet-induced dyslipidemia enhances the capacity of Treg cells to migrate towards sites of inflammation but that lipid accumulation in combination with the local environment inside atherosclerotic lesions is unfavourable for Treg cells, thereby disrupting their immunosuppressive capacity. In support of this, Treg cells inside murine atherosclerotic lesions become increasingly apoptotic as lesions progress during diet-induced atherosclerosis, an effect which is counteracted by restoration of normocholesterolemia.⁶ The main culprit lipoprotein in atherosclerosis is the cholesterol-rich LDL particle, which becomes oxidized in the vessel wall. oxLDL can dose-dependently induce apoptosis in human Treg cells³⁹ and has been suggested to induce apoptosis in murine Treg cells as well.⁹ This suggests that dyslipidemia itself contributes to a micro-environment inside lesions which is especially unfavourable for Treg cells.

Another feasible explanation for a loss of Treg cells inside lesions is that Treg cells might lose expression of FoxP3 inside atherosclerotic lesions and are therefore not identifiable as Treg cells. Indeed, oxLDL can increase methylation of the demethylated regions in the promoter of the *FoxP3* gene in Treg cells from healthy subjects,⁴⁰ thus decreasing *FoxP3* expression. Moreover, WTD-induced atherogenesis was shown to decrease FoxP3 expression in Treg cells and induce their differentiation to follicular helper T cells, which was partly mediated by membrane cholesterol accumulation.⁴¹ These reports indicate that the inflammatory phenotype is, in part, dictated by the intracellular lipid status of CD4⁺ T cells.

Figure 4 Continued

Slc25a20, *Plin2* and *Lipe* in NCD- and WTD-Treg cells. *n* = 6 mice/group. (C) Heatmap showing abundance of selected natural PPAR δ ligands from lipidomics screen in serum of NCD and WTD-fed mice. (D) Abundance of PPAR δ ligands from fatty acids subclass (*n* = 12 mice/group), (E) hydroxyeicosatetraenoic acid (HETE) and hydroxyoctadecadienoic acid (HODE) subclasses (*n* = 6 mice/group), (F) lysophosphatidylcholine subclass (*n* = 12 mice/group), and (G) prostaglandin subclass (*n* = 6 mice/group). (H) mRNA expression of PPAR δ target genes of NCD- and WTD-Treg cells after *in vitro* treatment with GSK0660 or vehicle. *n* = 5–7 mice/group. A two-tailed Student's *t*-test with a Bonferroni correction for multiple comparisons was used. Data from four groups were analysed using a one-way ANOVA. **P* < 0.05, ***P* < 0.01, ****P* < 0.001, *****P* < 0.0001. As C summarizes the data in D–G, the sample size corresponds to the sample size in D–G. In D–G, relative response indicates the abundance of each lipid species relative to its internal standard.

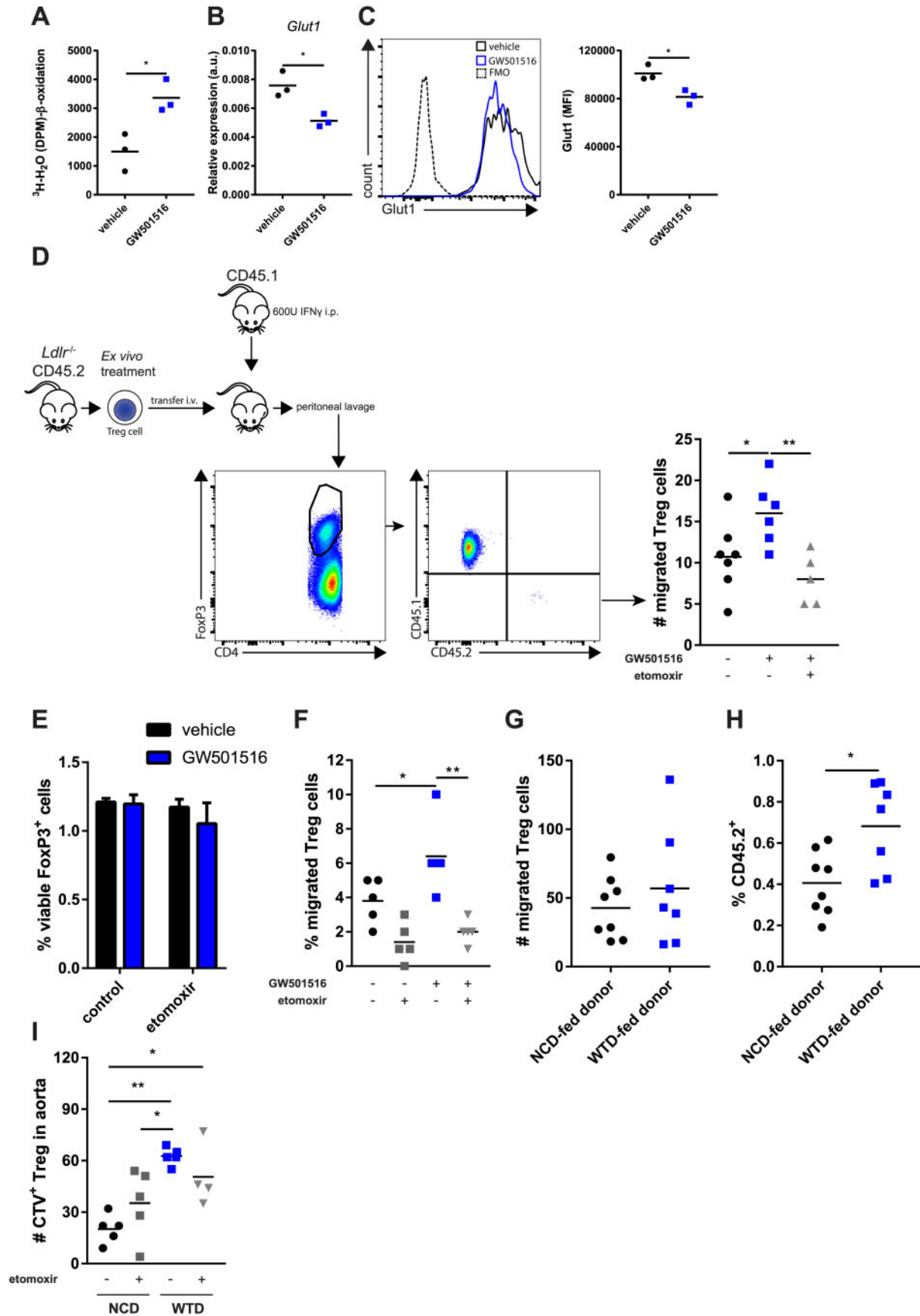


Figure 5 Increased FA oxidation increases *Ldlr*^{-/-} Treg cell migration. (A) ³H-palmitic acid detritiation in flow-sorted Treg cells treated with GW501516 in vivo. n = 3 mice/group. (B) *Glut1* mRNA expression in flow-sorted Treg cells treated with GW501516 in vitro. n = 3 mice/group. (C) *Glut1* protein

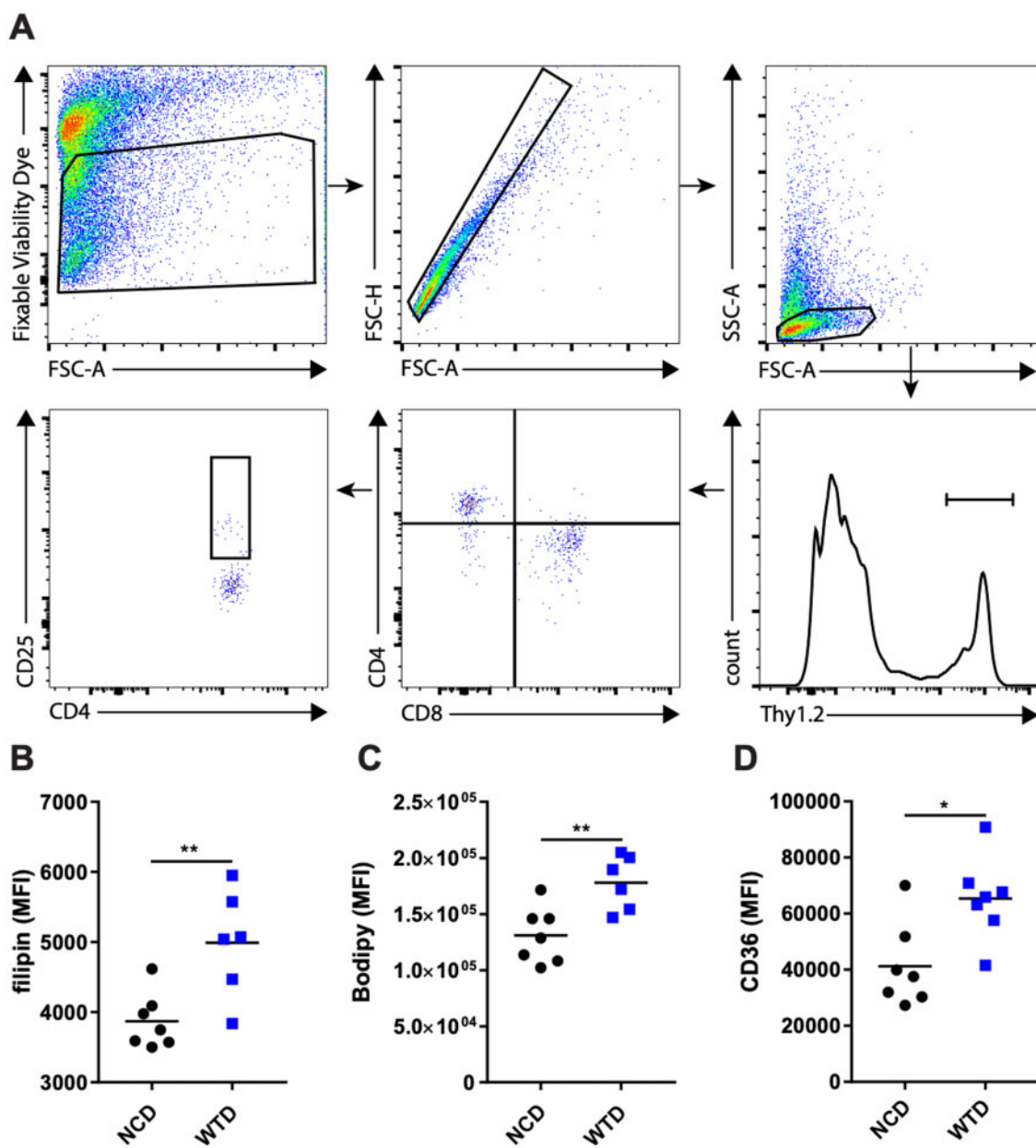


Figure 6 The effects of WTD-induced dyslipidemia on CD4⁺CD25^{hi} T cells in atherosclerotic lesions from *Ldlr*^{-/-} mice. (A) The representative gating strategy for CD4⁺CD25^{hi} T cells in digested atherosclerotic lesions microdissected from the aortic arch. (B) Filipin staining in CD4⁺CD25^{hi} T cells from A. *n* = 6–7 mice/group. (C) Bodipy staining in CD4⁺CD25^{hi} T cells from A. *n* = 6–7 mice/group. (D) CD36 staining in CD4⁺CD25^{hi} T cells from A. A two-tailed Student's *t*-test was used. *n* = 7 mice/group. **P* < 0.05, ***P* < 0.01. The plots in A represent an example for the applied gating strategy used in B–D, as shown in one biological sample.

Figure 5 Continued

expression measured in Treg cells from A by flow cytometry. (D) Peritoneal homing experiment using isolated Treg cells treated with GW501516. *n* = 5–7 mice/group. (E) Viability of isolated Treg cells with indicated treatments. *n* = 3/group (mean ± standard deviation). (F) Transmigration of isolated Treg cells towards CCL21 *in vitro* after indicated pretreatments. *n* = 5 mice/group. (G) Peritoneal homing experiment of NCD- vs. WTD-Treg cells. CD4⁺ T cells from NCD or WTD mice were injected i.v. and the number of Treg cells retrieved from the peritoneum were normalized for the number of Treg cells present in each donor CD4⁺ fraction. *n* = 7–8 mice/group. (H) Percentage of transferred NCD- and WTD-Treg cells relative to total number of peritoneal Treg cells. *n* = 7–8 mice/group. (I) *In vitro* aortic homing assay of NCD-Treg cells vs. WTD-Treg cells with or without preincubation with 100 μM etomoxir. Treg cells were left to migrate towards atherosclerotic aortic arches from *Apoe*^{-/-} mice. *n* = 4–5 mice/group. A–C and E and F represent data of two of three independent experiments. D represents data from two pooled experiments which showed similar effects. G–I represents data from one experiment. A two-tailed Student's *t*-test and one-way ANOVA were used. **P* < 0.05 and ***P* < 0.01.

We showed that diet-induced dyslipidemia did not affect LN migration and FA oxidation in Tconv cells, suggesting that the migratory and metabolic adaptations we observed can be Treg cell-specific. We speculate that the difference in CD36 expression between Tconv and Treg cells might explain why the latter are more sensitive to perturbations in environmental lipid levels. Nevertheless, it would be interesting to metabolically characterize Tconv cells (Thelper cell subsets) in SLOs and atherosclerotic lesions as their response to dyslipidemia will depend on the metabolic demand and differ among subsets. Data from previous reports suggest that dyslipidemia contributes to a microenvironment in lesions which is especially hostile for Treg cells, indicating that decreased immunosuppression by Treg cells in atherosclerotic lesions is likely due to local apoptosis and differentiation to T helper cell subsets but not due to decreased migration of circulating Treg cells towards lesions.

Diet-induced dyslipidemia affected Treg cells differently depending on the tissue compartment we examined. Lipoproteins in the blood can infiltrate LNs through the high-endothelial venules or the lymphatics system. Presumably, the increase in Treg cells and their lipid content in the medLN might be explained by ongoing inflammation in atherosclerotic lesions and copious amounts of (modified) lipoproteins which may drain to the medLN. Splenic Treg cells are presumably more sensitive to circulating lipids as these lipids presumably enter the spleen more easily since it is a very well-vascularized SLO. Our findings that splenic Treg cells are affected by dyslipidemia are especially relevant since this population encounters blood-borne antigens (e.g. derived from modified LDL⁴²) and contains antigen-specific Treg cells during atherosclerosis.²⁹ We speculate that circulating Treg cells in WTD-fed *Ldlr*^{-/-} mice did not show enhanced lipid accumulation because circulating Treg cells represent a mixed population, consisting of cells recirculating between (lymphoid) tissues and the blood- and lymph compartments, and our results indicated that this phenomenon is not uniform across (lymphoid) tissues. Importantly, we did observe increased lipids in aortic Treg cells, though it is unlikely that, as opposed to the spleen, aortic CD4⁺CD25^{hi} T cells predominantly represent Treg cells as these can also be activated Tconv cells.

In the spleen, dyslipidemia led to elevated cholesterol in Treg cells which decreased mTORC1 activity and led to decreased expression of genes from the mevalonate pathway. Endocytosis of lipoproteins could have resulted in large amounts of cholesterol in lysosomes which are sensed by mTORC1. Lysosomal cholesterol accumulation can specifically activate the mTORC1 complex through the SLC38A9–Niemann-Pick C1 signalling complex.⁴³ Instead, our data suggested cholesterol overload in Treg cells decreased mTORC1 activity. This is also supported by literature describing Treg cell-specific genetic deletion of *Abcg1* in mice with normolipidemia and dyslipidemia resulted in an increase in free cholesterol levels and decreased mTORC1 activity in Treg cells.¹² Interestingly, a recent report described that PPAR δ activation in natural killer cells can limit mTORC1-regulated glycolysis,⁴⁴ suggesting that, although we presume it is the main mechanism, inhibition of mTORC1 *in vivo* might not be exclusively mediated by cholesterol accumulation.

Dyslipidemia increased the mitochondrial FA oxidation rate and reversion to normolipidemia through dietary intervention abolished this effect, suggesting that systemic lipid metabolism is tightly linked to cellular lipid metabolism in Treg cells. Although glycolysis and glycolytic capacity were slightly impaired, increased ATP generation through FA oxidation might have compensated for decreased glycolysis when large amounts of ATP are required for cytoskeletal actin rearrangements during cell migration.^{45,46} In Treg cells, glucokinase has been shown to be

crucial for glycolysis-derived ATP generation to facilitate Treg cell migration upon migratory stimuli.¹¹ In our analyses, *Gck* mRNA expression was undetected in the majority of WTD-Treg cells (data not shown). However, the Treg cells used in the report describing *Gck* to be important for Treg cell migration were primarily generated or treated *in vitro* meaning that these cells probably depended mainly on glycolysis for ATP generation. In support of this, in CD8⁺ T cells, the ECAR dose-dependently increases with the concentration of glucose in the culture medium.⁴⁷ As dyslipidemia and GW501516 treatment augmented FA oxidation and migration, our study suggests that the dominant ATP-generating catabolic pathway is crucial for Treg cell migration and how bioenergetic metabolism is skewed by which environmental stimuli might determine which catabolic pathway is dominant. Pre-treatment of WTD-Treg cells with etomoxir had a smaller impact on migratory capacity than in GW501516-treated Treg cells, suggesting that WTD-Treg cells might be more flexible in switching to alternative catabolic pathways to generate ATP. Of note, the reported metabolic adaptations might coincide with a changed repertoire of chemokine receptors and/or selectin molecules beyond the ones we examined, as mTORC1 regulates many facets of T cell migration,⁴⁸ thus warranting further investigation. In addition, the link between dyslipidemia-induced changes in FA metabolism and Treg cell function warrants further investigation as Treg cell function is altered by metabolic immunomodulation¹⁹ but we observed no apparent differences in immunosuppression in WTD-Treg cells. Since literature has described a WTD to have no effect⁶ or increase Treg cell function *in vitro*⁴⁹ in different models of dyslipidemia this suggests a complex link between dyslipidemia, metabolism and Treg cell function.

We speculate that the concept of dietary lipids modulating Treg cell metabolism and migration is of particular interest to FH, as dyslipidemia can be quite severe in these patients. The most common germline mutations causing FH are in the *LDLr*, *APOE*, or *PCSK9* gene.⁵⁰ Treg cells from patients with mutations in either of the latter two have a functional LDL receptor, potentially resulting in even more lipoprotein uptake than FH patients with loss-of-function mutations in the *LDLr* gene. Interestingly, a recent study reporting comprehensive lipid profiling in children showed that non-statin-treated FH children have increased serum levels of DHA, linoleic acid and polyunsaturated FA as compared to non-FH children.⁵¹ This indicates that dyslipidemia in FH patients might lead to PPAR δ activation in human Treg cells and that cellular metabolism might be affected through similar mechanisms as described in our study.

There are some limitations to this study. We described that dyslipidemia was associated with changes in mTORC1 and PPAR δ activity in WTD-Treg cells and metabolic adaptations. However, it remains unclear whether and how these are linked and what the relative contributions of mTORC1 and PPAR δ are to the dyslipidemia-induced alterations in glycolysis and FA metabolism. Using a Treg cell-specific knock-out model for *Raptor* to study the contribution of mTORC1 inhibition to the observed metabolic phenotype is problematic as *Raptor*-deficient Treg cells are metabolically distinct from wildtype Treg cells.¹⁹ The exact contribution of PPAR δ in our studies can be examined in mice with Treg cell-specific PPAR δ deficiency, although Treg cells from these mice might have distinct glycolytic- and FA metabolism from wildtype Treg cells without dietary intervention, possibly affecting the effect of dietary intervention.

Altogether, our observations suggest that dietary lipids can alter Treg cell metabolism and migratory function. This indicates that pharmacological intervention to increase Treg cell migration alone might not suffice to dampen atherosclerosis or other autoimmune-like diseases if the microenvironment at the site of inflammation is not suitable for Treg cells.

Supplementary material

Supplementary material is available at *Cardiovascular Research* online.

Authors' contributions

J.A. and J.K. conceptualized and designed the work. J.A., F.H.S., H.D., P.J.v.S., G.H.M.v.P., B.S., A.C.F., E.M., I.B., and Y.W. acquired data for the work. J.A., E.M., A.H., T.H., H.C., I.B., and J.K. contributed to the analysis and/or interpretation of data for the work.

Conflict of interest: none declared.

Funding

This work was supported by European Union's Seventh Framework [grant number 603131], by contributions from Academic and SME/industrial partners to H.D. and F.S. and by the Netherlands Heart Foundation [grant number 2016T008] to A.C.F. and grant number CVON2017-20. H.C. was supported by the NIH [grant numbers, AI131703, AI150241, and AI150514].

Data availability

The complete mass spectrometry lipidomics screen as reported in the study is available in the Dryad repository through <https://doi.org/10.5061/dryad.70rxwdbv0>.

References

- Libby P, Lichtman AH, Hansson GK. Immune effector mechanisms implicated in atherosclerosis: from mice to humans. *Immunity* 2013;**38**:1092–1104.
- Goldberg AC, Hopkins PN, Toth PP, Ballantyne CM, Rader DJ, Robinson JG, Daniels SR, Gidding SS, Ferranti S, D, Ito MK, McGowan MP, Moriarty PM, Cromwell WC, Ross JL, Ziajka PE. Familial Hypercholesterolemia: screening, diagnosis and management of pediatric and adult patients. *J Clin Lipidol* 2011;**5**:S1–S8.
- Hopkins PN, Toth PP, Ballantyne CM, Rader DJ. Familial hypercholesterolemias: prevalence, genetics, diagnosis and screening recommendations from the National Lipid Association Expert Panel on Familial Hypercholesterolemia. *J Clin Lipidol* 2011;**5**: S9–S17.
- Buckner JH. Mechanisms of impaired regulation by CD4+CD25+FOXP3+ regulatory T cells in human autoimmune diseases. *Nat Rev Immunol* 2010;**10**:849–859.
- Boehmer HV, Daniel C. Therapeutic opportunities for manipulating TReg cells in autoimmunity and cancer. *Nat Rev Drug Discov* 2013;**12**:51–63.
- Maganto-Garcia E, Tarrío ML, Grabie N, Bu D.-X, Lichtman AH. Dynamic changes in regulatory T cells are linked to levels of diet-induced hypercholesterolemia. *Circulation* 2011;**124**:185–195.
- Boer OJ, de Meer JJ, V D, Teeling P, Loos CVD, Wal AVD. Low numbers of FOXP3 positive regulatory T cells are present in all developmental stages of human atherosclerotic lesions. *PLoS One* 2007;**2**:e779.
- Dietel B, Cicha I, Voskens CJ, Verhoeven E, Achenbach S, Garlisch CD. Decreased numbers of regulatory T cells are associated with human atherosclerotic lesion vulnerability and inversely correlate with infiltrated mature dendritic cells. *Atherosclerosis* 2013;**230**:92–99.
- Mor A, Luboshits G, Planer D, Keren G, George J. Altered status of CD4+CD25+ regulatory T cells in patients with acute coronary syndromes. *Eur Heart J* 2006;**27**: 2530–2537.
- Mauro C, Smith J, Cucchi D, Coe D, Fu H, Bonacina F, Baragetti A, Cermenati G, Caruso D, Mitro N, Catapano AL, Ammirati E, Longhi MP, Okkenhaug K, Norata GD, Marelli-Berg FM. Obesity-induced metabolic stress leads to biased effector memory CD4+ T cell differentiation via PI3K p110 δ -Akt-mediated signals. *Cell Metab* 2017;**25**:593–609.
- Kishore M, Cheung KCP, Fu H, Bonacina F, Wang G, Coe D, Ward EJ, Colamattéo A, Jangani M, Baragetti A, Matarese G, Smith DM, Haas R, Mauro C, Wraith DC, Okkenhaug K, Catapano AL, De Rosa V, Norata GD, Marelli-Berg FM. Regulatory T cell migration is dependent on glucokinase-mediated glycolysis. *Immunity* 2017;**47**: 875–889.e10.
- Cheng H-Y, Gaddis DE, Wu R, McSkimming C, Haynes LD, Taylor AM, McNamara CA, Sorci-Thomas M, Hedrick CC. Loss of ABCG1 influences regulatory T cell differentiation and atherosclerosis. *J Clin Invest* 2016;**126**:3236–3246.
- Shi LZ, Wang R, Huang G, Vogel P, Neale G, Green DR, Chi H. HIF1 α -dependent glycolytic pathway orchestrates a metabolic checkpoint for the differentiation of TH17 and Treg cells. *J Exp Med* 2011;**208**:1367–1376.
- Wang R, Dillon CP, Shi LZ, Milasta S, Carter R, Finkelstein D, McCormick LL, Fitzgerald P, Chi H, Munger J, Green DR. The transcription factor Myc controls metabolic reprogramming upon T lymphocyte activation. *Immunity* 2011;**35**:871–882.
- DeBerardinis RJ, Lum JJ, Thompson CB. Phosphatidylinositol 3-kinase-dependent modulation of carnitine palmitoyltransferase 1A expression regulates lipid metabolism during hematopoietic cell growth. *J Biol Chem* 2006;**281**:37372–37380.
- Um SH, Frigerio F, Watanabe M, Picard F, Joaquin M, Sticker M, Fumagalli S, Allegrini PR, Kozma SC, Auwerx J, Thomas G. Absence of S6K1 protects against age- and diet-induced obesity while enhancing insulin sensitivity. *Nature* 2004;**431**:200–205.
- Bensinger SJ, Tontonoz P. Integration of metabolism and inflammation by lipid-activated nuclear receptors. *Nature* 2008;**454**:470–477.
- Raud B, Roy DG, Divakaruni AS, Tarasenko TN, Franke R, Ma EH, Samborska B, Hsieh WY, Wong AH, Stüve P, Arnold-Schrauf C, Guderian M, Lochner M, Rampertaap S, Romito K, Monsale J, Brönstrup M, Bensinger SJ, Murphy AN, McGuire PJ, Jones RG, Sparwasser T, Berod L. Etomoxir actions on regulatory and memory T cells are independent of Cpt1 α -mediated fatty acid oxidation. *Cell Metab* 2018;**28**: 4–515.
- Zeng H, Yang K, Cloer C, Neale G, Vogel P, Chi H. mTORC1 couples immune signals and metabolic programming to establish T(reg)-cell function. *Nature* 2013;**499**: 485–490.
- Fu H, Kishore M, Gittens B, Wang G, Coe D, Komarowska I, Infante E, Ridley AJ, Cooper D, Perretti M, Marelli-Berg FM. Self-recognition of the endothelium enables regulatory T-cell trafficking and defines the kinetics of immune regulation. *Nat Commun* 2014;**5**: 3436.
- Li J, McArdle S, Gholami A, Kimura T, Wolf D, Gerhardt T, Miller J, Weber C, Ley K. CCR5+ T-bet+ FoxP3+ effector CD4 T cells drive atherosclerosis. *Circ Res* 2016;**118**:1540–1552.
- Hu C, Dommelen JV, Heijden RVD, Spijksma G, Reijmers TH, Wang M, Slee E, Lu X, Xu G, Greef JVD, Hankemeier T. RPLC-Ion-Trap-FTMS method for lipid profiling of plasma: method validation and application to p53 mutant mouse model. *J Proteome Res* 2008;**7**:4982–4991.
- Strassburg K, Huijbrechts AML, Kortekaas KA, Lindeman JH, Pedersen TL, Dane A, Berger R, Brenkman A, Hankemeier T, van Duynhoven J, Kalkhoven E, Newman JW, Vreeken RJ. Quantitative profiling of oxylipins through comprehensive LC-MS/MS analysis: application in cardiac surgery. *Anal Bioanal Chem* 2012;**404**:1413–1426.
- Chi H. Regulation and function of mTOR signalling in T cell fate decisions. *Nat Rev Immunol* 2012;**12**:325–338.
- Akimova T, Beier UH, Wang L, Levine MH, Hancock WW. Helios expression is a marker of T cell activation and proliferation. *PLoS One* 2011;**6**:e24226.
- Peterson TR, Sengupta SS, Harris TE, Carmack AE, Kang SA, Balderas E, Guertin DA, Madden KL, Carpenter AE, Finck BN, Sabatini DM. mTOR complex 1 regulates Lipin 1 localization to control the SREBP pathway. *Cell* 2011;**146**:408–420.
- Düvel K, Yecies JL, Menon S, Raman P, Lipovsky AI, Souza AL, Triantafellow E, Ma Q, Gorski R, Cleaver S, Vander Heiden DG, MacKeigan JP, Finan PM, Clish CB, Murphy LO, Manning BD. Activation of a metabolic gene regulatory network downstream of mTOR complex 1. *Mol Cell* 2010;**39**:171–183.
- Eid W, Dauner K, Courtney KC, Gagnon A, Parks RJ, Sorisky A, Zha X. mTORC1 activates SREBP-2 by suppressing cholesterol trafficking to lysosomes in mammalian cells. *Proc Natl Acad Sci USA* 2017;**114**:7999–8004.
- Klingenberg R, Lebens M, Hermansson A, Fredrikson GN, Strothoff D, Rudling M, Ketelhuth DJF, Gerdes N, Holmgren J, Nilsson J, Hansson GK. Intranasal immunization with an apolipoprotein B-100 fusion protein induces antigen-specific regulatory T cells and reduces atherosclerosis. *Arterioscler Thromb Vasc Biol* 2010;**30**:946–952.
- Cunningham JT, Rodgers JT, Arlow DH, Vazquez F, Mootha VK, Puigserver P. mTOR controls mitochondrial oxidative function through a YY1-PGC-1 α transcriptional complex. *Nature* 2007;**450**:736–740.
- Procaccini C, Carbone F, Di Silvestre D, Brambilla F, De Rosa V, Galgani M, Faicchia D, Marone G, Tramontano D, Corona M, Alviggi C, Porcellini A, La Cava A, Mauri P, Matarese G. The proteomic landscape of human ex vivo regulatory and conventional T cells reveals specific metabolic requirements. *Immunity* 2016;**44**:406–421.
- Libby P, Ridker PM, Maseri A. Inflammation and atherosclerosis. *Circulation* 2002;**105**: 1135–1143.
- Fan W, Waizenegger W, Lin CS, Sorrentino V, He M-X, Wall CE, Li H, Little C, Yu RT, Atkins AR, Auwerx J, Downes M, Evans RM. PPAR δ promotes running endurance by preserving glucose. *Cell Metab* 2017;**25**:1186–1193.e4.
- Cipolletta D, Feuerer M, Li A, Kamei N, Lee J, Shoelson SE, Benoist C, Mathis D. PPAR- γ is a major driver of the accumulation and phenotype of adipose tissue Treg cells. *Nature* 2012;**486**:549–553.
- Nahlé Z, Hsieh M, Pietka T, Coburn CT, Grimaldi PA, Zhang MQ, Das D, Abumrad NA. CD36-dependent regulation of muscle FoxO1 and PDK4 in the PPAR δ / β -mediated adaptation to metabolic stress. *J Biol Chem* 2008;**283**:14317–14326.
- Chawla A, Lee C-H, Barak Y, He W, Rosenfeld J, Liao D, Han J, Kang H, Evans RM. PPAR δ is a very low-density lipoprotein sensor in macrophages. *Proc Natl Acad Sci USA* 2003;**100**:1268–1273.

37. Kahremany S, Livne A, Gruzman A, Senderowitz H, Sasson S. Activation of PPAR δ : from computer modelling to biological effects: binding parameters of PPAR δ activators. *Br J Pharmacol* 2015;**172**:754–770.
38. Klingler C, Zhao X, Adhikary T, Li J, Xu G, Häring H-U, Schleicher E, Lehmann R, Weigert C. Lyso-phosphatidylcholines activate PPAR δ and protect human skeletal muscle cells from lipotoxicity. *Biochim Biophys Acta* 2016;**1861**:1980–1992.
39. Zhang W, Wang J, Shu Y, Tang T, Zhu Z, Xia N, Nie S, Liu J, Zhou S, Li J, Xiao H, Yuan J, Liao M, Cheng L, Liao Y, Cheng X. Impaired thymic export and increased apoptosis account for regulatory T cell defects in patients with non-ST segment elevation acute coronary syndrome. *J Biol Chem* 2012;**287**:34157–34166.
40. Jia L, Zhu L, Wang JZ, Wang XJ, Chen JZ, Song L, Wu YJ, Sun K, Yuan ZY, Hui R. Apolipoprotein AI prevents regulatory T cells is related to the severity of coronary artery disease. *Atherosclerosis* 2013;**228**:346–352.
41. Gaddis DE, Padgett LE, Wu R, McSkimming C, Romines V, Taylor AM, McNamara CA, Kronenberg M, Crotty S, Thomas MJ, Sorci-Thomas MG, Hedrick CC. Apolipoprotein AI prevents regulatory to follicular helper T cell switching during atherosclerosis. *Nat Commun* 2018;**9**.
42. Palinski W, Hörkö S, Miller E, Steinbrecher UP, Powell HC, Curtiss LK, Witztum JL. Cloning of monoclonal autoantibodies to epitopes of oxidized lipoproteins from apolipoprotein E-deficient mice. Demonstration of epitopes of oxidized low density lipoprotein in human plasma. *J Clin Invest* 1996;**98**:800–814.
43. Castellano BM, Thelen AM, Moldavski O, Feltes M, van der Welle REN, Mydock-McGrane L, Jiang X, van Eijkeren RJ, Davis OB, Louie SM, Perera RM, Covey DF, Nomura DK, Ory DS, Zoncu R. Lysosomal cholesterol activates mTORC1 via an SLC38A9–Niemann-Pick C1 signaling complex. *Science* 2017;**355**:1306–1311.
44. Michelet X, Dyck L, Hogan A, Loftus RM, Duquette D, Wei K, Beyaz S, Tavakkoli A, Foley C, Donnelly R, O'Farrelly C, Raverdeau M, Vernon A, Pettee W, O'Shea D, Nikolajczyk BS, Mills KHG, Brenner MB, Finlay D, Lynch L. Metabolic reprogramming of natural killer cells in obesity limits antitumor responses. *Nat Immunol* 2018;**19**:1330–1340.
45. Bernstein BW, Bamberg JR. Actin-ATP hydrolysis is a major energy drain for neurons. *J Neurosci* 2003;**23**:1–6.
46. Pantaloni D, Le Clainche C, Carlier M-F. Mechanism of actin-based motility. *Science* 2001;**292**:1502–1506.
47. Blagih J, Coulombe F, Vincent EE, Dupuy F, Galicia-Vázquez G, Yurchenko E, Raissi TC, van der Windt GJW, Viollet B, Pearce EL, Pelletier J, Piccirillo CA, Krawczyk CM, Divangahi M, Jones RG. The energy sensor AMPK regulates T cell metabolic adaptation and effector responses in vivo. *Immunity* 2015;**42**:41–54.
48. Finlay D, Cantrell DA. Metabolism, migration and memory in cytotoxic T cells. *Nat Rev Immunol* 2011;**11**:109–117.
49. Møller RKW, Gisterå A, Polyzos KA, Ketelhuth DFJ, Hansson GK. Hypercholesterolemia enhances T cell receptor signaling and increases the regulatory T cell population. *Sci Rep* 2017;**7**:15655.
50. Besseling J, Sjouke B, Kastelein J. Screening and treatment of familial hypercholesterolemia—lessons from the past and opportunities for the future (based on the Anitschkow Lecture 2014). *Atherosclerosis* 2015;**241**:597–606.
51. Christensen JJ, Ulven SM, Retterstøl K, Narverud I, Bogsrud MP, Henriksen T, Bollerslev J, Halvorsen B, Aukrust P, Holven KB. Comprehensive lipid and metabolite profiling of children with and without familial hypercholesterolemia: a cross-sectional study. *Atherosclerosis* 2017;**266**:48–57.

Translational perspective

Dyslipidemia, in the form of hypercholesterolemia and hypertriglyceridemia, is a driver of atherosclerosis and cardiovascular disease (CVD). Hence, lipid-lowering therapy is a cornerstone in the treatment of CVD. In the past years, the clinical feasibility of immunotherapy to treat CVD has also been established. As regulatory T (Treg) cells are specialized in immunosuppression, these cells represent a promising target for additional immunotherapies. The presented study suggests that dyslipidemia affects the metabolism of Treg cells and their migration towards sites of inflammation, such as atherosclerotic lesions, suggesting that lipid-lowering therapy and metabolic immunotherapy might affect Treg cells through previously unidentified mechanisms.